JACS
JOURNAL OF THE AMERICAN CHEMICAL SOCIETY
Article
pubs.acs.org/JACS

Light- and Heat-Triggered Reversible Linear−Cyclic Topological Conversion of Telechelic Polymers with Anthryl End Groups

Takuya Yamamoto,*[,†,‡] Sakyo Yagyu,[†] and Yasuyuki Tezuka[†]

[†]Department of Organic and Polymeric Materials, Tokyo Institute of Technology, O-okayama, Meguro-ku, Tokyo 152−8552, Japan
[‡]Division of Applied Chemistry, Faculty of Engineering, Hokkaido University, Sapporo, Hokkaido 060−8628, Japan

Supporting Information

ABSTRACT: This study demonstrates the comprehensive investigation on the reversible linear−cyclic topological conversion of hydrophilic and hydrophobic polymers with various molecular weights. The reactions were triggered by light or heat, which reversibly dimerize and cleave the anthryl or coumarinyl end groups of the telechelics. Poly(ethylene oxide) telechelics with anthryl end groups attached through electron-donating (**Ant−O−PEO** and **Ant−CH_2−PEO**) and electron-withdrawing (**Ant−CO_2−PEO**) linking groups were synthesized. While **Ant−O−PEO** and **Ant−CH_2−PEO** decomposed upon photoirradiation at 365 nm, **Ant−CO_2−PEO** efficiently cyclized through the photodimerization of the anthryl end groups both in water and in organic solvents shown by NMR, SEC, and MALDI-TOF MS. The lower the molecular weight, the faster the cyclization proceeded. When cyclized **Ant−CO_2−PEO** was heated at 150 °C in bulk, the polymers quantitatively converted back into the original linear topology. Furthermore, repeatable linear−cyclic topological conversion was confirmed. The reversible topological conversion of hydrophobic poly(tetrahydrofuran) telechelics with anthryl end groups (**Ant−PTHF**) was also successful. In addition, poly(ethylene oxide) telechelics with coumarinyl end groups (**Cou−PEO**) were also cyclized by irradiation at 365 nm in water. However, the cyclization hardly occurred when performed in methanol likely due to the lack of sufficient hydrophobic interaction of the coumarinyl end groups. Cyclized **Cou−PEO** was irradiated at 254 nm to test for linearization, finding the linear product and cyclic precursor were likely photoequilibrated.

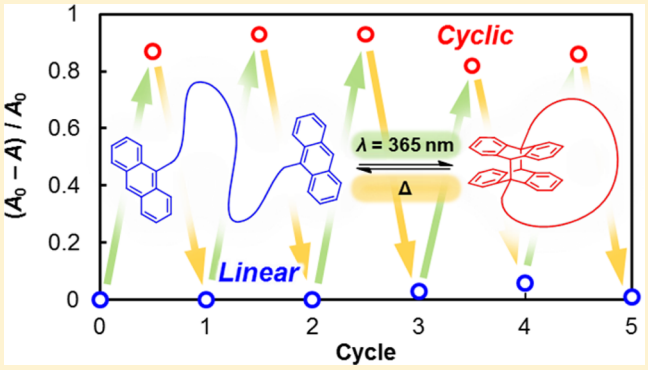

INTRODUCTION

In recent years, the advances in polymer chemistry have made it possible to synthesize polymers possessing various topologies.[1] Examples of those include star-shaped, hyperbranched, and ladder-shaped polymers, to mention a few. Among the many shapes, cyclic polymers are receiving a lot of attention with its unique topology, and a variety of cyclization methods have been invented.[2−7] As cyclic polymers do not have any ends, they have different physical properties, such as a smaller hydrodynamic volume, higher glass transition temperature, and lower viscosity, when compared to linear polymers having the same composition and molecular weight.[8] The effects stemming from the topology of the polymer are known as *topology effects*, and those effects of various cyclic polymers are being examined.[9]

Topology effects receive much attention in recent years, and there are many studies are appearing in the literature on this subject. Research topics include the differences that were observed in the diffusion behavior in single molecule measurements,[10] controllability of domain spacing in block copolymer phase separation,[11] the crystallization rate,[12−14] the melting point,[15] gel properties,[16] and the rheology of the melt state[17] to cite a few. Grayson synthesized linear and cyclic poly(ε-caprolactone) and examined the acid-catalyzed degeneration of these polymers.[18] The rate of degeneration was tracked using SEC and MALDI-TOF MS, and they reported that the degeneration of the cyclic polymers was slower than its linear counterpart. It has also been reported that when poly((2-dimethylamino)ethyl methacrylate) was tested as a polycation gene carrier and its DNA transfection efficiency was examined, the cyclic form had a higher delivery efficiency and lower cytotoxicity.[19] We reported on the *topology effects* of amphiphilic copolymers, which had poly(ethylene oxide) on its hydrophilic segment and poly(alkyl acrylate) on its hydrophobic segments. When the amphiphilic linear triblock copolymer and its corresponding cyclized diblock copolymer were compared for its cloud point and salting-out effect, it was found that the cyclic form acquires a higher heat and salt tolerance.[20]

Thus, it was thought that if the polymer topology conversion process is repeatedly reversible, and its various *topology effects* are controlled, it could prove to be quite interesting for novel materials development. However, such repeatedly reversible

Received: January 22, 2016
Published: February 26, 2016

DOI: 10.1021/jacs.6b00800
J. Am. Chem. Soc. 2016, 138, 3904−3911

Scheme 1. (a) Reversible Topological Transformation of Ant−O−PEO, Ant−CH_2−PEO, Ant−CO_2−PEO, and Ant−PTHF by Irradiation at 365 nm and Heating; (b) Reversible Topological Transformation of Cou−PEO by Irradiation at 365 and 254 nm

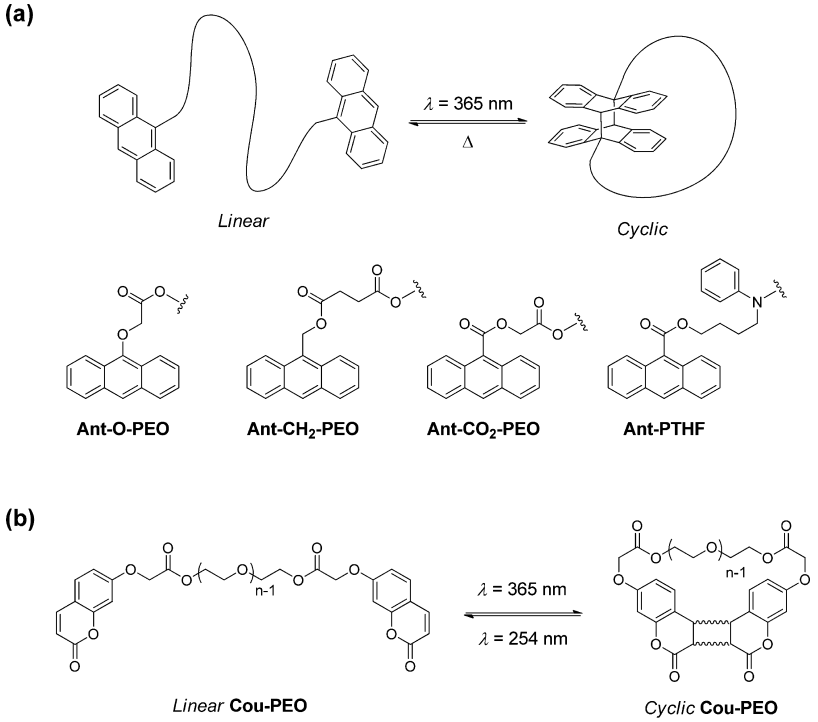

topological conversion is difficult and reports on its success are limited to only one system, using iron porphyrin on the chain ends of polystyrene.[21,22] Cyclization occurs upon changing the acid/base conditions. Under basic conditions, porphyrin−porphyrin coupling takes place through an oxygen atom while in acidic conditions a reverse reaction occurs to linearize the polymer. Thus, the addition of an acid and a base controls the polymer topology. The redox reaction of thiol end groups is potentially applicable for repeatedly reversible linear−cyclic topological conversion by the addition of oxidizing and reducing agents.[23,24] However, only one cycle (linear-to-cyclic-to-linear) was experimentally demonstrated due to practical difficulties. Nevertheless, industrial and environmental issues are involved in these processes due to the use of reagents, including a metal reducing agent, and the accumulation of byproducts in the system. Thus, the use of "clean" and convenient reactions are desired. In this regard, several light-induced cyclization reactions were recently reported.[25−30] Among these, there is a study claiming the synthesis of cyclic poly(ε-caprolactone) through dimerizing anthracene.[31] However, this report did not achieve the cyclization of a single polymer chain, and the reverse reaction only partially proceeded (46%).

In this study, we appended anthracene or coumarin to the ends of poly(ethylene oxide), PEO, and poly(tetrahydrofuran), PTHF, with various molecular weights and conducted a comprehensive examination on the reversible topological conversion process with light and heat (Scheme 1). Anthracene is known to dimerize via a [4 + 4] cycloaddition reaction when irradiated with light with a wavelength greater than 340 nm.[32] When exposed to light under 300 nm, it undergoes a photocleavage reaction. An anthracene dimer can be cleaved by heat as well. This thermal cleavage reaction uses less activation energy than the photocleavage reaction. Based on these facts, we believe that it should be possible to create a durable and reversible cyclic and linear topological conversion process by using anthracene as the end groups. Thus, we synthesized three derivatives of 9-substituted anthracene with electron-donating (**Ant−O−PEO** and **Ant−CH_2−PEO**) and electron-withdrawing (**Ant−CO_2−PEO**) linking groups to the main chain for the optimization of the reactions, achieving repeatedly reversible topological conversion (Scheme 1a). Coumarin exhibits photoreactivity analogous to that of anthracene. It dimerizes by irradiation of light with a wavelength higher than 310 nm.[33,34] When the dimer is exposed to a wavelength less than 290 nm, it cleaves and reverts to a monomer state. For this study, 7-oxycoumarin was selected as the coumarin derivative to be used at the termini (**Cou−PEO**), as it is easily obtained and exhibits good photodimerization reactivity (Scheme 1b).[35] Concerning the molecular weight, shorter polymer chains should lead to faster cyclization. Moreover, it was expected that cyclic polymers are effectively obtained in a polar solvent by taking advantage of the hydrophobic and $\pi-\pi$ interactions of anthryl and coumarinyl end groups.

RESULTS AND DISCUSSION

Synthesis of Poly(Ethylene Oxide) with Anthryl End Groups (Ant−O−PEO, Ant−CH_2−PEO, and Ant−CO_2−PEO). PEO with anthryl end groups was synthesized by a condensation reaction between hydroxy-terminated PEO and anthracene derivatives bearing a carboxylic acid functional group (Scheme S1). In this study, we synthesized three types of anthracene derivatives with electron-donating (**Ant−O−PEO** and **Ant−CH_2−PEO**) and electron-withdrawing (**Ant−CO_2−PEO**) substituents at the 9-position based on the functional group directly attaching to the anthryl group. The reason for selecting the position of the substituents for this study was that the dimer in this case has only two bonding modes (head-to-

DOI: 10.1021/jacs.6b00800
J. Am. Chem. Soc. 2016, 138, 3904−3911

head and head-to-tail), which would be easier to analyze by NMR.

Ant−O−PEO was synthesized by the esterification of the hydroxy end groups of PEO with 9-anthracenyloxyacetic acid in the presence of 1-ethyl-3-(3-(dimethylamino)propyl)carbodiimide hydrochloride (EDAC) as a condensing agent and *N*,*N*-dimethyl-4-aminopyridine (DMAP) as a catalyst (Scheme S1a, Figures S1 and S2).[36] The molecular weight of the PEO was 3 kDa (**Ant−O−PEO$_{3k}$**) and 10 kDa (**Ant−O−PEO$_{10k}$**). Similarly, **Ant−CH$_2$−PEO** was synthesized by the esterification of the hydroxy end groups of PEO with 4-(anthracen-9-ylmethoxy)-4-oxobutanoic acid[37] in the presence of EDAC and DMAP (Scheme S1b, Figures S3−S5). The molecular weight of the PEO was 3 kDa (**Ant−CH$_2$−PEO$_{3k}$**). For the synthesis of **Ant−CO$_2$−PEO**, 2-((anthracene-9-carbonyl)oxy)acetic acid was first prepared using TFA to deprotect the *tert*-butyl group in 2-(*tert*-butoxy)-2-oxoethylanthracene-9-carboxylate (Scheme S1c). Esterification was performed with hydroxy-terminated PEO in the presence of EDAC and DMAP to give **Ant−CO$_2$−PEO$_{3k}$** and **Ant−CO$_2$−PEO$_{10k}$**. From the ^{1}H NMR spectra after the reaction, the signal "g" from the methylene protons adjacent to the ester group appeared, which confirms the esterification (Figure S6). All other signals were also attributed to the respective protons. The SEC charts were unimodal (Figure S7), and with MALDI-TOF MS, only the intended product with both ends functionalized was observed (Figure S8). Thus, we were able to confirm that the reaction had progressed quantifiably successfully, synthethically yielding the intended telechelics.

Synthesis of PTHF with Anthryl End Groups (Ant−PTHF). PTHF with anthryl end groups was synthesized via the electrostatic self-assembly and covalent fixation process as given in Scheme S2.[38] PTHF with *N*-phenylpyrrolidinium end groups was subjected to a counterion exchange with sodium anthracene-9-carboxylate to form an ionic complex (Figure S9), which was then refluxed in dilution to form covalent bonds, giving **Ant−PTHF$_{4k}$** and **Ant−PTHF$_{12k}$**. These telechelics were characterized by ^{1}H NMR (Figure S10), SEC (Figure S11), and MALDI-TOF-MS (Figure S12)

Synthesis of Poly(Ethylene Oxide) with Coumarinyl End Groups (Cou−PEO). In accordance with Scheme S3, the linear polymer was synthesized through the condensation reaction between 7-coumariloxyacetic acid and hydroxy-terminated PEO with three different molecular weights in the presence of EDAC and DMAP. The characterization of the resulting polymers (**Cou−PEO$_{3k}$**, **Cou−PEO$_{6k}$**, and **Cou−PEO$_{10k}$**) was performed with ^{1}H NMR (Figure S13), SEC (Figure S14), and MALDI-TOF-MS (Figure S15).

Reversible Topological Conversion of Ant−O−PEO, Ant−CH$_2$−PEO, and Ant−CO$_2$−PEO. First, we examined the cyclization of **Ant−CH$_2$−PEO$_{3k}$** by irradiating a 0.2 g/L aqueous solution (5 mg of the polymer dissolved in 25 mL of water) with 365 nm wavelength light. From the UV−vis spectra, the absorption of 365 nm light reduced over time, and the results indicated that the anthryl end groups photoreacted (Figure S16). However, no signal for the anthracene dimer was observed in the ^{1}H NMR spectra after irradiation (Figure S17). Instead the anthryl groups were oxidized to form anthraquinone. From the missing "f" signal, we can presume that the anthryl groups broke away from the chain ends of PEO to form anthraquinone. Interestingly, this result is different from the one recently reported on a poly(ε-caprolactone) main chain with anthryl end groups having the same linking manner between the anthryl groups and the main chain.[31] In the study, macrocyclization was reportedly successful by two or more units of the telechelics, while no formation of a unimeric cyclic polymer was found. **Ant−O−PEO$_{10k}$** also generated anthraquinone through oxidation upon irradiation (Figure S18). Conceivably, when the solution was irradiated, dissolved oxygen may have been excited, and singlet molecular oxygen was created from triplet oxygen. This singlet molecular oxygen would undergo a Diels−Alder reaction with the anthracene derivative through an oxygenated intermediate,[39] which then converted to anthraquinone (Scheme S4).[40] The reactivity of the diene in the Diels−Alder reaction here can vary greatly based on the substituent present on the molecule. On one hand, if the substituent is electron withdrawing, then this reactivity should be significantly reduced. On the other hand, if the substituent is electron donating, the reactivity in the cycloaddition would increase. Therefore, the reason that **Ant−O−PEO** and **Ant−CH$_2$−PEO** oxidized to anthraquinone was likely because the reactivity of the diene was increased by the electron-donating substituent at the 9-position. Hence, by introducing a strongly electron-withdrawing substituent at the 9-position, the Diels−Alder reaction would be avoided toward the initially designed photodimerization process.

Thus, 0.2 g/L of **Ant−CO$_2$−PEO$_{3k}$** or **Ant−CO$_2$−PEO$_{10k}$**, possessing electron-withdrawing substituents, was prepared as an aqueous solution, a methanol solution, or a toluene solution, and each system was examined for cyclization by irradiation with 365 nm wavelength light. The photodimerization reaction of anthracene was tracked by the absorbance at 365 nm using UV−vis spectroscopy, and the progress of the dimerization reaction was estimated by the proportion of the decrease in the absorbance with respect to its original value before irradiation, i.e., $(A_0 - A)/A_0$. The reaction showed good progress in 10 min when the molecular weight was 3 kDa and 30 min when the molecular weight was 10 kDa (Figures 1, 2, S19, and S20). The

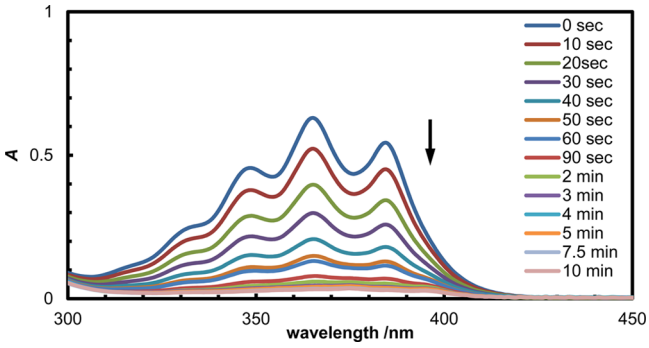

Figure 1. Time-course UV−vis spectra of **Ant−CO$_2$−PEO$_{3k}$** upon irradiation at 365 nm for cyclization in water.

reason behind this is thought to be the hydrophobic and π−π interactions, which did not significantly help to hold two anthryl end groups together for dimerization when the molecular weight of PEO became higher. When the rate of the photodimerization reaction in various solvent was compared, the results were as follows: in water > in toluene > in methanol (Figure 2). The reason for water having the fastest rate could be the reinforced hydrophobic and π−π interactions in the polar environment. From the ^{1}H NMR, signals for the anthracene dimer appeared after the irradiation and were found to comprise head-to-tail dimers (Figure 3). Furthermore, the peak *m*/*z* values did not change when the

DOI: 10.1021/jacs.6b00800
J. Am. Chem. Soc. 2016, 138, 3904−3911

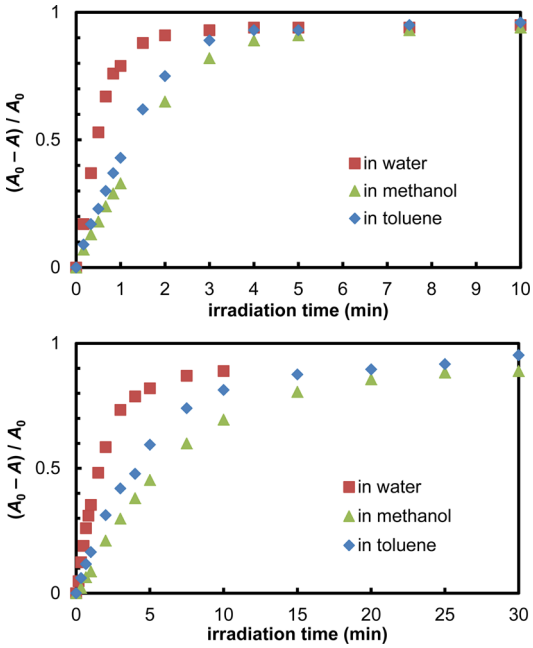

Figure 2. $(A_0 - A)/A_0$ at 365 nm versus time plots for cyclization by irradiation at 365 nm. (Top) **Ant−CO_2−PEO_{3k}** and (bottom) **Ant−CO_2−PEO_{10k}**.

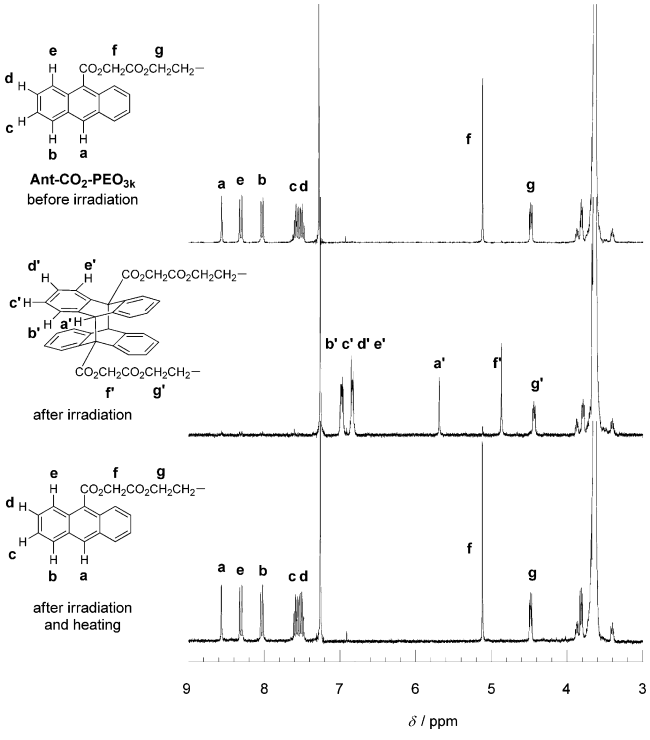

Figure 3. ^{1}H NMR spectra of **Ant−CO_2−PEO_{3k}** (top) before irradiation, (middle) after irradiation at 365 nm for 10 min in water, and (bottom) after irradiation at 365 nm for 10 min in water and heating at 150 °C for 2 h in bulk under vacuum.

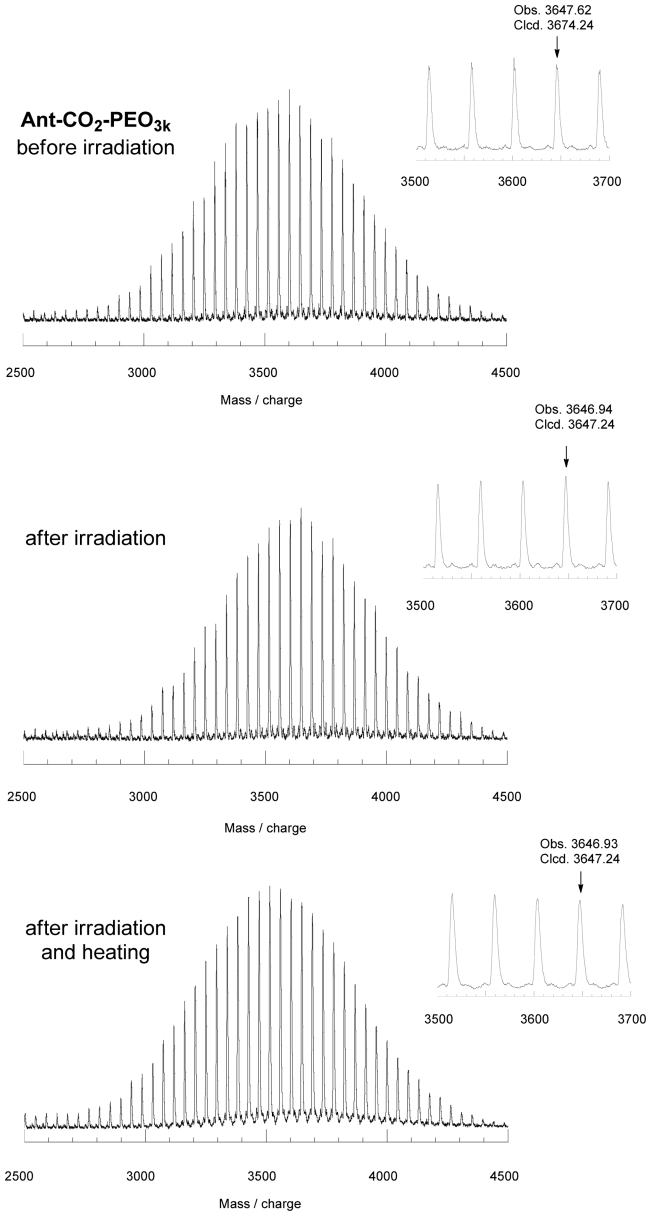

Figure 4. MALDI-TOF mass spectra of **Ant−CO_2−PEO_{3k}** (top) before irradiation, (middle) after irradiation at 365 nm in water for 10 min, and (bottom) after irradiation at 365 nm in water for 10 min and heating at 150 °C for 2 h in bulk under vacuum.

samples were evaluated with MALDI-TOF MS, suggesting no decomposition (Figures 4 and S21). With SEC measurements, the peak top molecular weight decreased after the irradiation in all the solvents (Figures 5 and S22), and no linear precursor remained. The SEC chart also shows a peak, which likely indicates the intermolecularly reacted two units of the telechelics. This could be due to the ambient light causing a slight reversible reaction. Therefore, we removed this peak component by using preparative SEC and immediately measured the sample with analytical SEC, but unfortunately, the peak appeared again. We consider that the reason for the formation of the intermolecularly reacted products is because these polymers could form aggregates like micelles.

On examining linearization through the thermal cleavage reaction, the signals for the anthracene monomer reappeared after heating at 150 °C for 2 h in bulk under vacuum (Figure 3). The peak top molecular weight did increase, and a profile similar to that for the original linear polymer was obtained (Figures 5e and S22e). When MALDI-TOF MS was performed, the linearized forms exhibited mass spectra with the same m/z values as those before irradiation and after irradiation at 365 nm, and the calculated molecular weight and

DOI: 10.1021/jacs.6b00800
J. Am. Chem. Soc. 2016, 138, 3904−3911

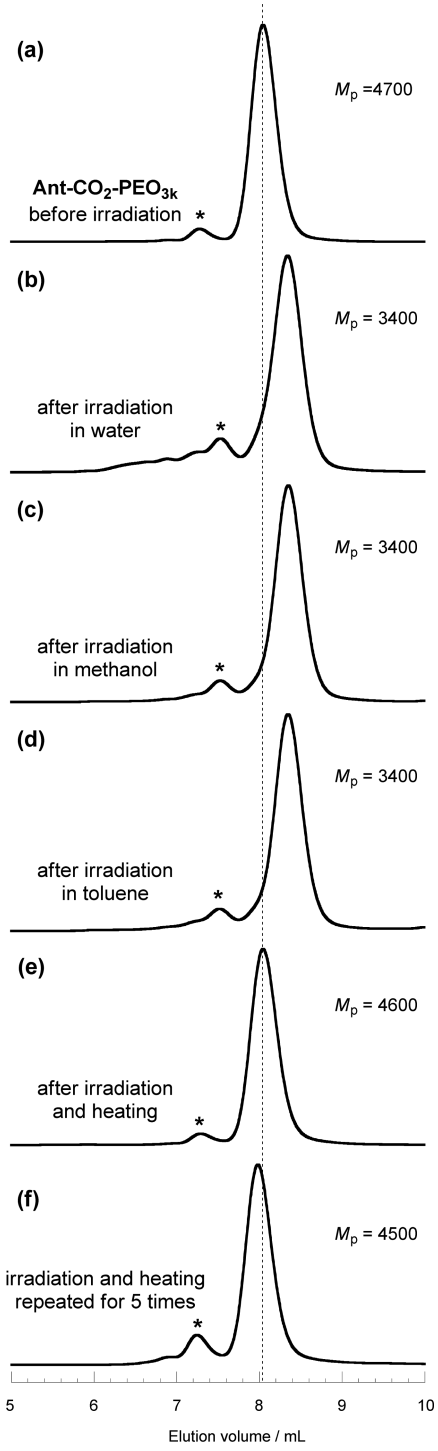

Figure 5. SEC charts of **Ant−CO_2−PEO_{3k}** (a) before irradiation, (b) after irradiation at 365 nm in water for 10 min, (c) after irradiation at 365 nm in methanol for 15 min, (d) after irradiation at 365 nm in toluene for 10 min, (e) after irradiation in water for 10 min and heating at 150 °C for 2 h in bulk under vacuum, and (f) with irradiation and heating repeated for 5 times. Asterisk likely indicates the intermolecularly reacted two units of the telechelics under ambient light conditions.

the observed molecular weight showed a very good match (Figures 4 and S21). Furthermore, after repeating photodimerization and thermal cleavage five times and subsequently analyzing through SEC, we found that the original peak shape with **Ant−CO_2−PEO_{3k}** was maintained intact for the most part (Figures 5f and 6).

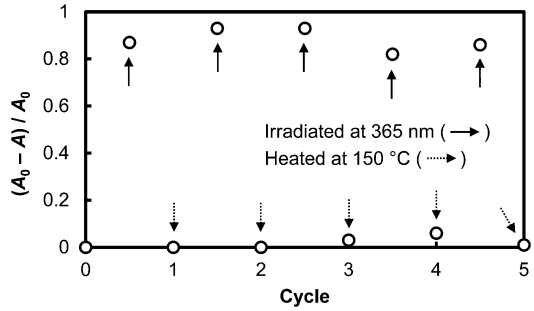

Figure 6. $(A_0 - A)/A_0$ of **Ant−CO_2−PEO_{3k}** at 365 nm upon repeating irradiation and heating cycles.

Reversible Topological Conversion of Ant−PTHF. In anticipation of the possibility of making a hydrophobic polymer for a reversible topological transformation similar to the case of the hydrophilic polymers, an anthryl group was added to the ends of poly(tetrahydrofuran) (PTHF). Thus, a methanol solution with 0.2 g/L of **Ant−$PTHF_{4k}$** was prepared and irradiated with 365 nm wavelength light to examine for cyclization. When the reaction was tracked with UV−vis spectra just as in **Ant−CO_2−PEO**, the dimerization was complete within 2 to 3 h (Figure 7). We were also able to verify this

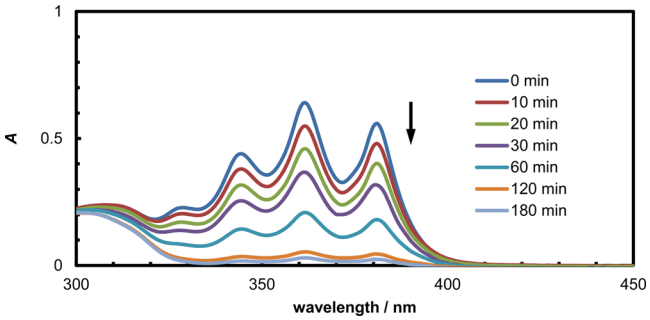

Figure 7. Time-course UV−vis spectrum of **Ant−$PTHF_{4k}$** upon irradiation at 365 nm for cyclization in methanol.

through ^{1}H NMR spectra as the signals from the anthracene dimer appeared (Figure 8). SEC measurements revealed that the peak top molecular weight also decreased, which meant that a topological conversion took place from the linear to the cyclic state (Figure 9). Following this, we attempted linearization through a thermal cleavage reaction. As described previously, heat (150 °C) was applied for 2 h in bulk, and the anthracene monomer signal reappeared in the ^{1}H NMR spectra (Figure 8). The peak top molecular weight also increased in the SEC experiment, verifying that linearization indeed occurred (Figure 9).

Ant−$PTHF_{12k}$ did not fully dissolve in methanol; thus, a methanol/dichloromethane (9/1) mixed solvent was prepared. **Ant−$PTHF_{12k}$** was dissolved to generate a solution at 0.2 g/L, which was subsequently irradiated with a 365 nm wavelength light to cyclize the telechelics. A decrease in the peak top molecular weight was shown by SEC measurements, which confirmed that the cyclization progressed (Figure S23). Following this, linearization through a thermal cleavage reaction was attempted. The peak top molecular weight in

DOI: 10.1021/jacs.6b00800
J. Am. Chem. Soc. 2016, 138, 3904−3911

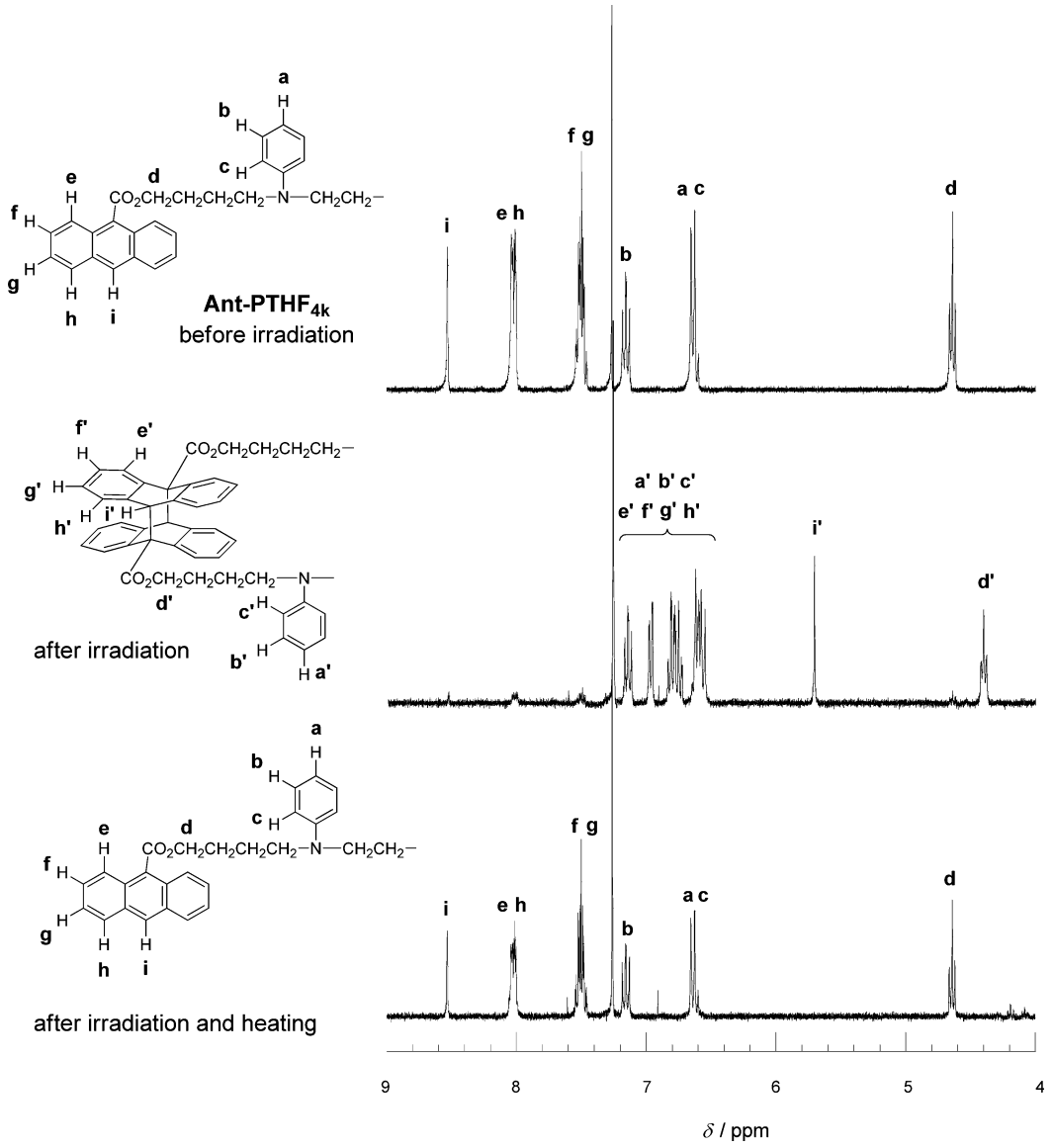

Figure 8. ^{1}H NMR spectra of **Ant−PTHF$_{4k}$** (top) before irradiation, (middle) after irradiation at 365 nm in methanol for 3 h, and (bottom) after irradiation at 365 nm in methanol for 3 h and heating at 150 °C in bulk for 2 h.

SEC increased, and it matched the original linear state of the polymer. However, the SEC profile was not symmetrical, which indicated the presence of some intermolecularly reacted products in the system. The reasons for this observation are the basis of further studies.

Reversible Topological Conversion of Cou−PEO. The reversible topological conversion of synthesized PEO with coumarinyl end groups (**Cou−PEO**) was also tested through cyclization by irradiation with 365 nm wavelength light and subsequent linearization by irradiation with 254 nm wavelength light. Thus, a 0.2 g/L aqueous solution of **Cou−PEO$_{3k}$**, **Cou−PEO$_{6k}$**, or **Cou−PEO$_{10k}$** was prepared and irradiated at 365 nm. The progression of the coumarin photodimerization reaction was followed by UV−vis spectroscopy. The polymer end groups contained a 7-oxycoumarin structure, which is known to show absorbance of light at a wavelength of 320 nm that disappears upon dimerization.[33] Thus, the progress of the dimerization reaction was estimated by $(A_0 - A)/A_0$ at 320 nm, shown in Figures S24−S26. In NMR spectra, the "a" and "b" signals from the olefin proton disappeared, and the "a′" and "b′" signals from the cyclobutane structure appeared instead (Figure S27). The "c", "d", and "e" signals also shifted.[33] The rate of the reaction depended on the molecular weight. The smaller the molecular weight, the faster the dimerization reaction was. When the molecular weight was 10 kDa, it required approximately 24 h for $(A_0 - A)/A_0$ to reach 0.8 (Figure S26). On the other hand, **Cou−PEO$_{3k}$** required only 3 h to exceed 0.9. This trend is the same as that for **Ant−CO$_2$−PEO**. In the cases of **Cou−PEO$_{3k}$** and **Cou−PEO$_{6k}$**, the peak top molecular weight in the SEC chromatograms decreased (Figures S28 and S29). As the results were unimodal, we believe that the topological conversion toward a cyclic form took place. However, in the case of **Cou−PEO$_{10k}$**, though the results showed that the peak top molecular weight lowered, there were still linear chains remaining in the sample (Figure S30). The reason for the presence of the linear PEO chains is that, as mentioned above, the hydrophobic and $\pi-\pi$ interactions contribute less at higher molecular weights. MALDI-TOF MS also showed that spectra after cyclization were nearly identical to those in the linear form, and the

DOI: 10.1021/jacs.6b00800
J. Am. Chem. Soc. 2016, 138, 3904−3911

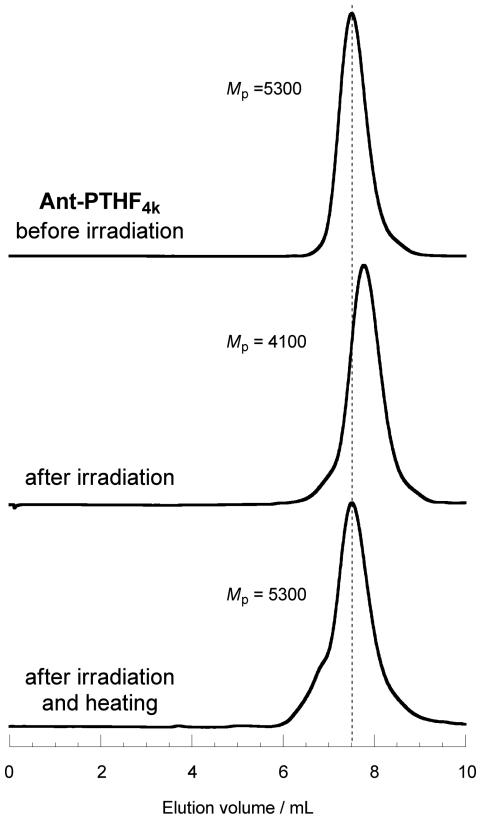

Figure 9. SEC charts of **Ant−PTHF$_{4k}$** (top) before irradiation, (middle) after irradiation at 365 nm for 3 h in methanol, and (bottom) after irradiation at 365 nm for 3 h in methanol and heating at 150 °C in bulk for 2 h.

calculated and observed m/z values matched very well (Figure S31). From this result, the reduction in the peak top molecular weight in the SEC experiments was confirmed not because the main chain decomposed, but rather because the topology transformed from a linear state to a cyclic state.

In contrast, when the samples were irradiated at 365 nm in methanol, we found that although some chains cyclized, most of **Cou−PEO** remains in the linear form (Figure S32). This is because the hydrophobic and $\pi-\pi$ interactions are significantly weakened in methanol, and thus, the coumarinyl ends do not get close enough to one another, slowing down the progression of the photodimerization reaction. When the molecular weight effects on this phenomenon were analyzed, we find that the lower the molecular weight, the more effective the cyclization was. This is likely because when the molecular weight is lower, the distance between the coumarinyl end groups become shorter which speeds up the photodimerization process. These results are consistent with the case of **Ant−CO$_2$−PEO**.

Cyclized **Cou−PEO$_{6k}$** was irradiated in water with 254 nm wavelength light to examine linearization through the cleavage reaction of the coumarin dimer. We also tracked the cleavage reaction through an increase in the absorbance at 320 nm. The $(A_0 - A)/A_0$ value, where A_0 is the absorbance before irradiation at 365 nm, was 0.65 after 30 min of irradiation at 254 nm, but beyond that, no matter how long the irradiation continued, no further progression in the reaction was observed (Figure S24). When comparing the ^{1}H NMR spectra before and after irradiation, the signal for the coumarin dimer became weaker while the signal for the coumarin monomer reappeared (Figure S27). The molecular weight of the products was verified by MALDI-TOF MS (Figure S33). Moreover, the peak top molecular weight value increased in each of the samples as measured by SEC (Figures S28−S30). By these results, we confirmed that some degree of the cyclic-to-linear conversion took place. However, the SEC profiles were not unimodal, which indicate that the samples still contained a significant amount of the cyclic polymer precursor and intermolecularly reacted products. This result could be attributed to the fact that the photocleavage reaction was at equilibrium with the photodimerization reaction.

CONCLUSIONS

The present study demonstrates that by the use of PEO telechelics with anthryl end groups connected through an electron-withdrawing functionality at the 9 position, cyclic polymers were efficiently and easily constructed in both water and organic solvents. Heating the cyclized polymers regenerated the original linear telechelics. By combining these two processes, we established a highly durable reversible topological conversion. Furthermore, this methodology was applicable to hydrophobic PTHF main chains.

Such repeatedly reversible topological conversion processes for controlling topology effects would lead to the discovery of novel polymeric materials. The unimeric cyclization using anthracene is an easier and more economical process than those that have been reported to date. As this process does not use reagents, purification is not required. We believe that this could greatly contribute toward the synthesis of cyclic polymers and in the search and discovery of novel material properties.

ASSOCIATED CONTENT

Supporting Information

The Supporting Information is available free of charge on the ACS Publications website at DOI: 10.1021/jacs.6b00800.

Experimental section, synthetic and photooxidation schemes, ^{1}H NMR spectra, SEC charts, MALDI-TOF mass spectra, time-course UV−vis spectra, and $(A_0 - A)/A_0$ versus time plots (PDF)

AUTHOR INFORMATION

Corresponding Author

*yamamoto.t@eng.hokudai.ac.jp

Notes

The authors declare no competing financial interest.

ACKNOWLEDGMENTS

The authors are grateful to Prof. M. Kakimoto for access to measurement facilities. This work was supported by KAKENHI (26288099 T.Y., 15H01595 T.Y., and 15K13703 T.Y.).

REFERENCES

(1) *Topological Polymer Chemistry: Progress of Cyclic Polymers in Syntheses, Properties and Functions*; Tezuka, Y., Ed.; World Scientific: Singapore, 2013.
(2) Endo, K. *Adv. Polym. Sci.* **2008**, *217*, 121−183.
(3) Guo, L.; Zhang, D. *J. Am. Chem. Soc.* **2009**, *131*, 18072−18074.
(4) Kricheldorf, H. R. *J. Polym. Sci., Part A: Polym. Chem.* **2010**, *48*, 251−284.
(5) Hoskins, J. N.; Grayson, S. M. *Polym. Chem.* **2011**, *2*, 289−299.
(6) Jia, Z.; Monteiro, M. J. *J. Polym. Sci., Part A: Polym. Chem.* **2012**, *50*, 2085−2097.
(7) Zhu, Y.; Hosmane, N. S. *ChemistryOpen* **2015**, *4*, 408−417.

DOI: 10.1021/jacs.6b00800
J. Am. Chem. Soc. 2016, 138, 3904−3911

(8) Semlyen, J. A. *Cyclic Polymers*, 2nd ed.; Kluwer Academic Publishers: New York, 2002.
(9) Yamamoto, T.; Tezuka, Y. *Soft Matter* **2015**, *11*, 7458−7468.
(10) Habuchi, S.; Fujiwara, S.; Yamamoto, T.; Tezuka, Y. *Polym. Chem.* **2015**, *6*, 4109−4115.
(11) Poelma, J. E.; Ono, K.; Miyajima, D.; Aida, T.; Satoh, K.; Hawker, C. J. *ACS Nano* **2012**, *6*, 10845−10854.
(12) Tezuka, Y.; Ohtsuka, T.; Adachi, K.; Komiya, R.; Ohno, N.; Okui, N. *Macromol. Rapid Commun.* **2008**, *29*, 1237−1241.
(13) Kitahara, T.; Yamazaki, S.; Kimura, K. *Kobunshi Ronbunshu* **2011**, *68*, 694−701.
(14) Su, H.-H.; Chen, H.-L.; Díaz, A.; Casas, M. T.; Puiggalí, J.; Hoskins, J. N.; Grayson, S. M.; Pérez, R. A.; Müller, A. *Polymer* **2013**, *54*, 846−859.
(15) Bielawski, C. W.; Benitez, D.; Grubbs, R. H. *Science* **2002**, *297*, 2041−2044.
(16) Zhang, K.; Lackey, M. A.; Cui, J.; Tew, G. N. *J. Am. Chem. Soc.* **2011**, *133*, 4140−4148.
(17) Doi, Y.; Matsubara, K.; Ohta, Y.; Nakano, T.; Kawaguchi, D.; Takahashi, Y.; Takano, A.; Matsushita, Y. *Macromolecules* **2015**, *48*, 3140−3147.
(18) Hoskins, J. N.; Grayson, S. M. *Macromolecules* **2009**, *42*, 6406−6413.
(19) Wei, H.; Chu, D. S. H.; Zhao, J.; Pahang, J. A.; Pun, S. H. *ACS Macro Lett.* **2013**, *2*, 1047−1050.
(20) Honda, S.; Yamamoto, T.; Tezuka, Y. *Nat. Commun.* **2013**, *4*, 1574.
(21) Schappacher, M.; Deffieux, A. *J. Am. Chem. Soc.* **2011**, *133*, 1630−1633.
(22) Schappacher, M.; Deffieux, A. *Macromolecules* **2011**, *44*, 4503−4510.
(23) Whittaker, M. R.; Goh, Y.-K.; Gemici, H.; Legge, T. M.; Perrier, S.; Monteiro, M. J. *Macromolecules* **2006**, *39*, 9028−9034.
(24) Stamenović, M. M.; Espeel, P.; Baba, E.; Yamamoto, T.; Tezuka, Y.; Du Prez, F. E. *Polym. Chem.* **2013**, *4*, 184−193.
(25) Josse, T.; Altintas, O.; Oehlenschlaeger, K. K.; Dubois, P.; Gerbaux, P.; Coulembier, O.; Barner-Kowollik, C. *Chem. Commun.* **2014**, *50*, 2024−2026.
(26) Tang, Q.; Wu, Y.; Sun, P.; Chen, Y.; Zhang, K. *Macromolecules* **2014**, *47*, 3775−3781.
(27) Sun, P.; Tang, Q.; Wang, Z.; Zhao, Y.; Zhang, K. *Polym. Chem.* **2015**, *6*, 4096−4101.
(28) Josse, T.; De Winter, J.; Altintas, O.; Dubois, P.; Barner-Kowollik, C.; Gerbaux, P.; Coulembier, O. *Macromol. Chem. Phys.* **2015**, *216*, 1227−1234.
(29) Zhu, W.; Li, Z.; Zhao, Y.; Zhang, K. *Macromol. Rapid Commun.* **2015**, *36*, 1987−1993.
(30) Ji, Z.; Li, Y.; Ding, Y.; Chen, G.; Jiang, M. *Polym. Chem.* **2015**, *6*, 6880−6884.
(31) Wang, H.; Zhang, L.; Liu, B.; Han, B.; Duan, Z.; Qi, C.; Park, D.-W.; Kim, I. *Macromol. Rapid Commun.* **2015**, *36*, 1646−1650.
(32) Bouas-Laurent, H.; Castellan, A.; Desvergne, J.-P.; Lapouyade, R. *Chem. Soc. Rev.* **2000**, *29*, 43−55.
(33) Trenor, S. R.; Long, T. E.; Love, B. J. *Macromol. Chem. Phys.* **2004**, *205*, 715−723.
(34) Trenor, S. R.; Shultz, A. R.; Love, B. J.; Long, T. E. *Chem. Rev.* **2004**, *104*, 3059−3078.
(35) Gnanaguru, K.; Ramasubbu, N.; Venkatesan, K.; Ramamurthy, V. *J. Org. Chem.* **1985**, *50*, 2337−2346.
(36) Molard, Y.; Bassani, D. M.; Desvergne, J.-P.; Moran, N.; Tucker, J. H. R. *J. Org. Chem.* **2006**, *71*, 8523−8531.
(37) Shi, Z.; Hau, S.; Luo, J.; Kim, T.-D.; Tucker, N. M.; Ka, J.-W.; Sun, H.; Pyajt, A.; Dalton, L.; Chen, A.; Jen, A. K.-Y. *Adv. Funct. Mater.* **2007**, *17*, 2557−2563.
(38) Oike, H.; Imamura, H.; Imaizumi, H.; Tezuka, Y. *Macromolecules* **1999**, *32*, 4819−4825.
(39) Balci, M. *Chem. Rev.* **1981**, *81*, 91−108.
(40) Baldwin, J. E.; Basson, H. H.; Krauss, H. *Chem. Commun.* **1968**, 984−985.

DOI: 10.1021/jacs.6b00800
J. Am. Chem. Soc. 2016, 138, 3904−3911